Relationship between crystalline structure of poly(3-hexylthiophene) blends and properties of organic thin-film transistors – a brief review*)

Dorota Chlebosz[1)], Łukasz Janasz[2)], Wojciech Pisula[2), 3)], Adam Kiersnowski[1), **)]

DOI: dx.doi.org/10.14314/polimery.2016.433

Abstract: Poly(3-hexythiophene) (P3HT) is one of the most extensively studied polymers for applications in organic thin-film transistors. Semicrystalline P3HT is a p-type semiconductor enabling applications in the unipolar organic field-effect transistors (OFETs). Blending P3HT with small molecular compounds can enhance the mobility of charge carriers in the OFET active layer. When small molecules reveal electron conductivity and their phase separation upon crystallization in the presence of P3HT results in formation of heterojunctions, the blends can be considered candidates for active layers in the ambipolar OFETs. Regardless of unipolar or ambipolar, the charge carrier transport always depends on the inherent properties of the polymer and small molecules as well as the crystalline structure and morphology (nanostructure) of the blends. This paper is a brief review of the recent findings regarding relationships between structure and properties of the active layers of P3HT and P3HT blends-based OFETs. Herein we discuss examples of blends of P3HT with, amongst others, perylene diimide derivatives, and discuss their OFET-related properties, like charge-carrier mobility, in relation to both crystalline structure of the blend components and blend morphology. Some key issues related to morphology control by changing layer formation conditions are also indicated in this paper.

Keywords: poly(3-hexylthiophene) (P3HT), polymer blends, organic thin-film transistors.

Wpływ struktury poli(3-heksylotiofenu) i jego mieszanin na właściwości organicznych tranzystorów polowych – krótki przegląd

Streszczenie: Poli(3-heksylotiofen) (P3HT) to semikrystaliczny polimer, charakteryzujący się przewodnictwem dziurowym (typu p), dzięki czemu jest stosowany w aktywnych warstwach organicznych tranzystorów polowych (ang. Organic Field-Effect Transistor, OFET). Badania prowadzone w ciągu ostatnich lat wykazały, że mieszanie P3HT z poliaromatycznymi substancjami małocząsteczkowymi może powodować zwiększenie ruchliwości nośników ładunku (dziur) w warstwie aktywnej OFET. Zastosowanie dwufazowych mieszanin P3HT z małocząsteczkowymi substancjami o przewodnictwie typu n (np. pochodnymi perylenodiimidów) umożliwia otrzymanie tranzystorów ambipolarnych, które można wykorzystać m.in. do wytworzenia układów komplementarnych. Niezależnie od rodzaju urządzenia – unipolarnego lub ambipolarnego – transport nośników ładunku zależy od właściwości użytych substancji oraz struktury krystalicznej i morfologii (nanostruktury) mieszanin. W niniejszej pracy, na podstawie przeglądu literatury, omówiono strukturę krystaliczną i morfologię przykładowych mieszanin P3HT. Ponadto, przedyskutowano relacje pomiędzy cechami strukturalnymi cienkich filmów otrzymanych z P3HT i jego mieszanin a właściwościami OFET.

Słowa kluczowe: poli(3-heksylotiofen) (P3HT), mieszaniny polimerowe, organiczne tranzystory cienkowarstwowe.

[1)] Wroclaw University of Technology, Polymer Engineering and Technology Division, Wybrzeże Wyspiańskiego 27, 50-370 Wroclaw, Poland.

[2)] Lodz University of Technology, Department of Molecular Physics, Żeromskiego 116, 90-924 Lodz, Poland.

[3)] Max Planck Institute for Polymer Research, Ackermannweg 10, 55128 Mainz, Germany.

*) Material contained in this article was presented at 58th Annual Scientific Meeting of the Polish Chemical Society, 21–25 September 2015, Gdansk, Poland.

**) Author for correspondence; e-mail: adam.kiersnowski@pwr.edu.pl

BASIC STRUCTURAL PROPERTIES AND CRYSTALLINITY OF POLY(3-HEXYLTHIOPHENE)

Poly(3-hexylthiophene) (P3HT, Fig. 1a) is a π-conjugated polymer with an all-aromatic backbone formed by thiophene units, each substituted by flexible hexyl side-chains [1, 2]. Synthesis of the regioregular P3HT was a subject of numerous studies [3–5]. Because of the asymmetric chemical structure, the monomer units of P3HT can be joined in two different configurations, namely head-to-tail (H-T) or head-to-head (H-H) (Fig. 1) [3]. The polymer in which all monomer units are connected in H-T

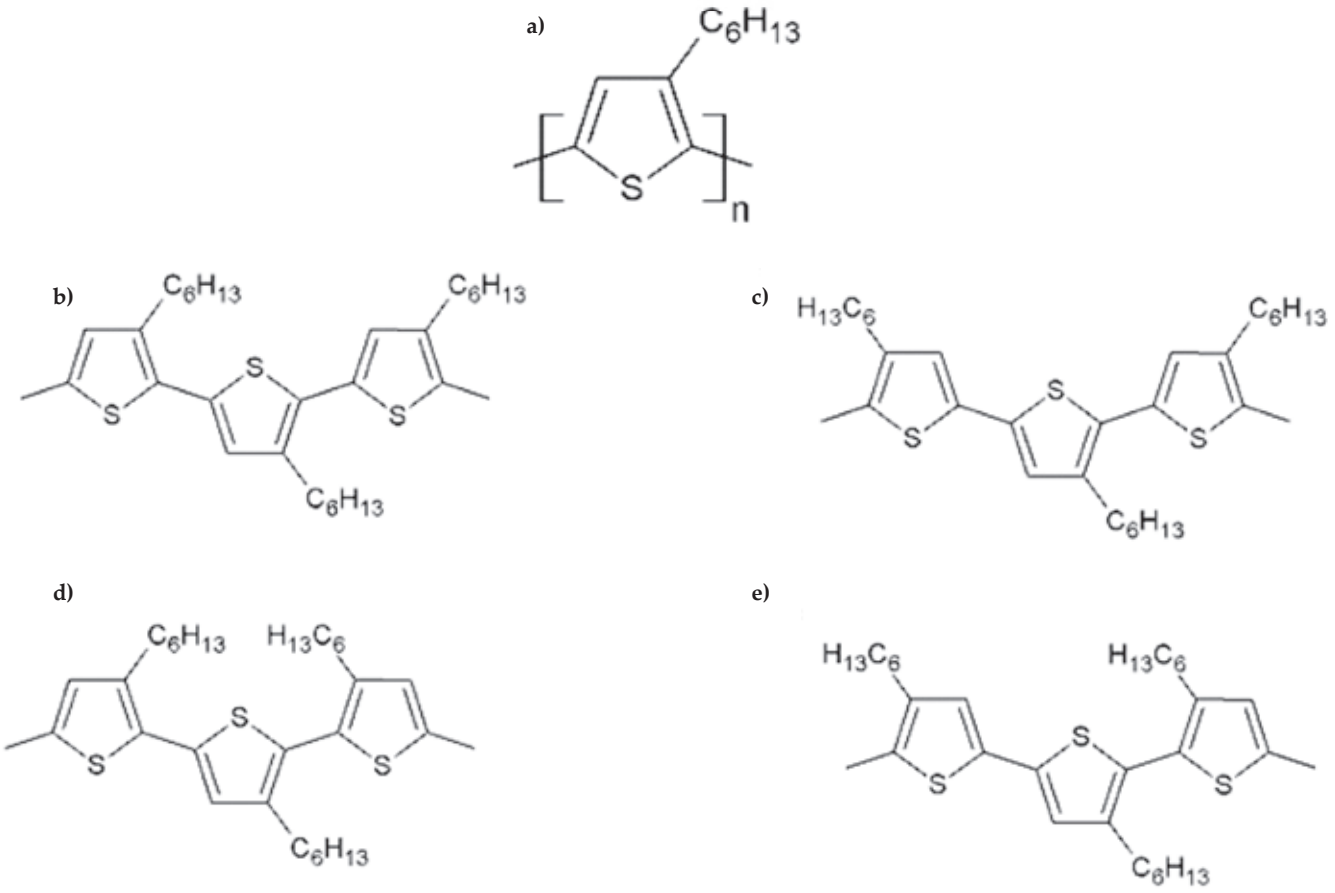

Fig. 1. Chemical structures of: a) P3HT, possible dyad configurations in P3HT chains b) head-tail-head-tail, c) tail-tail-head-tail, d) head-tail-head-head, e) tail-tail-head-head

configuration is called regioregular (Fig. 1b). P3HT with a random arrangement of H-H and H-T dyads (Fig. 1c–e) is referred to as regiorandom.

Solid P3HT is a semicrystalline polymer whose crystallinity index increases with increasing degree of regioregularity (RR) and depends also on the molar mass [6]. For example, the bulk crystallinity of P3HT with RR exceeding 98 % and weight average molar mass of 30 kg/mol (polydispersity = 1.6) can reach 60 wt % [6]. At 25 °C the crystalline structure of P3HT is dominated by a monoclinic polymorph, referred to as Form I (Fig. 2a) [7]. The main difference between the polymorphs is the ordering of hexyl side chains and tilting of the thiophene rings in the unit cell. The hexyl groups in the Form I are interdigitated with dominating *trans* dihedrals, while the backbones are spatially arranged with the $P2_1/c$ symmetry [6] (Fig. 2a). At 60 °C Form I reversibly transforms into Form II. This transition is manifested by an increase in mobility of the side chains which, however, are less mobile than in the amorphous P3HT. In the Form II the hexyl side chains are disordered, while the packing of main chains (Fig. 2b) reveals reduced or no symmetry [7, 8–11]. In both Forms I and II the thiophene rings of the neighboring P3HT chains are π-stacked leading to the formation of the characteristic layered structures in the P3HT crystalline domains. The Form I<>Form II transition can be detected by, for instance, differential scanning calorimetry (DSC) or solid-state NMR [7, 11].

The hexyl side-chains render P3HT soluble in common solvents, such as chloroform, chlorinated benzenes or toluene. In the laboratory the solubility allows processing of P3HT into the form of films by *e.g.* drop-casting, dip-, or spin-coating. P3HT can be also processed by more technologically relevant techniques such as ink-jet or screen printing. The crystallinity degree of P3HT films is often kinetically limited as the evaporation time of solvents is typically shorter than the time necessary to form well-developed crystals. To increase the crystallinity degree of the P3HT films, they are usually annealed (often in solvent vapor) below the melting point of the polymer (230 °C) [8, 12]. Highly crystalline P3HT films can be formed as a result of aggregation of the polymer in solution [8]. The aggregation can be induced by adding a thermodynamically poor solvent (*e.g.* anisole) to the solution of P3HT in a good solvent (as, *e.g.* chloroform) or conditioning the polymer solution by aging or UV-irradiation. The aggregates, typically fibrils or sometimes nodules [13], are formed via π-π interactions due to reduced solvation of the aromatic, conjugated main chains [8, 12]. The aggregation of P3HT in solution allows separating the crystallization process of P3HT from film deposition conditions [14].

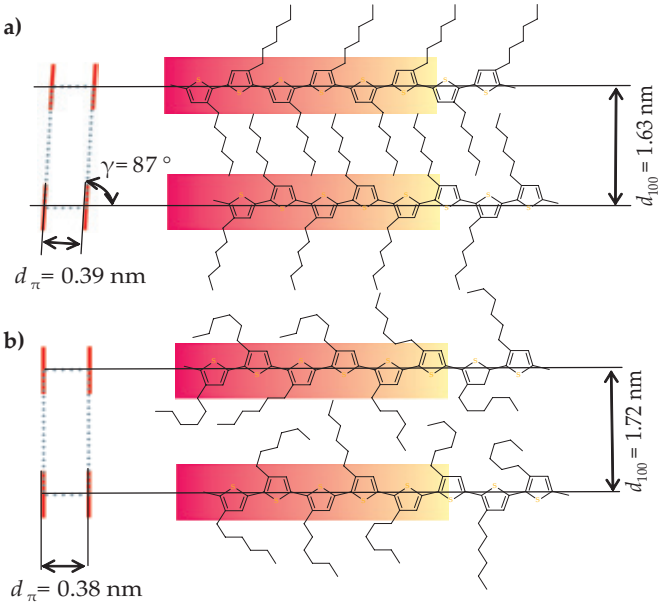

Fig. 2. Molecular packing in different crystalline polymorphs of P3HT: a) Form I, b) Form II; figures to the left show the geometry of the π-stacking in the crystalline cell as viewed along the axis of main chains schematically represented by red ribbons, d_{π} is the π-stacking distance in the crystalline units, while d_{100} is the average distance between the thiophene layers

P3HT macromolecules in thin films often orient on substrates in a preferential manner. The typical orientations are referred to as *edge-on* or *face-on* to depict the orientation of thiophene units toward the substrate surface (Fig. 3b–d) [15, 16]. Stable crystalline films with *edge-on* oriented P3HT chains (Fig. 3c) are usually formed during quasi-static evaporation of solvents [17, 18] The *edge-on* orientation is considered thermodynamically stable, while *face-on* oriented P3HT (Fig. 3b) is considered as a kinetically trapped metastable state [19]. The *face-on* orientation is observed for low RR P3HT or in films formed under shear [17]. Crystalline films in which the main axes of the P3HT backbones were perpendicular to the substrate (Fig. 3d) were also reported [8, 15, 16].

The π-electron system causes that P3HT, both in the solution and in a solid state, strongly absorbs light in the UV-visible range. Positions of the absorption bands depend, among others, on the main chain configuration. Regioregular P3HT absorbs wavelengths in the range 520––550 nm, while the absorption maximum of regiorandom P3HT is located at approx. 440 nm [20]. The π-conjugation along the backbone together with the π-stacking in the crystals turn P3HT into a semiconductor [21, 22] attractive for utilization in photovoltaics [23] and thin-film transistors [24]. The semiconductivity combined with the elastic modulus of P3HT (E_{P3HT} ~ 1.33 GPa [25]), similar to that of, for instance, polypropylene (E_{PP} ~ 1.5 GPa), opens the door towards applications in so-called *flexible electronics.*

POLY(3-HEXYLTHIOPHENE)-BASED ORGANIC FIELD-EFFECT TRANSISTORS

Field-effect transistors (FETs) are simple, but powerful devices to investigate the semiconducting properties of materials. FETs used to investigate the properties of semiconductors typically consist of two metal electrodes (source and drain), and a silicon gate electrode with silicon dioxide as a dielectric layer (Fig. 4). The film of the investigated semiconductor (the active layer) is deposited on top of the dielectric layer (Fig. 4). The currently reported charge carrier mobility for P3HT-based FETs is in the range between 0.1 to 1 $cm^2/V \cdot s$ [26, 27].

Electrical parameters of organic FETs (OFETs) are sensitive to inherent properties of the polymer, such as molar mass or regioregularity as well as crystallinity of the semiconducting layer. The intramolecular π-conjugation and intermolecular π-stacking of P3HT backbones allows charge carriers (holes) to be transported along the backbones and between neighboring chains respectively [28]. Basically, increasing the molar mass and the crystallinity both enhance the charge carrier mobility in OFET. We note, however, that the transport of charge carriers along the P3HT backbones is faster than chain-to-chain charge hopping, making the latter an important limiting factor for the OFET performance [28]. This is the reason why the electrical conductivity of P3HT with regioregularity (RR) exceeding 85 % is by 2–3 orders of magnitude higher than that of the regiorandom P3HT which reveals insufficient crystallinity and hence π-stacking density [3, 28]. The consequence of the charge transport through the π-stacks

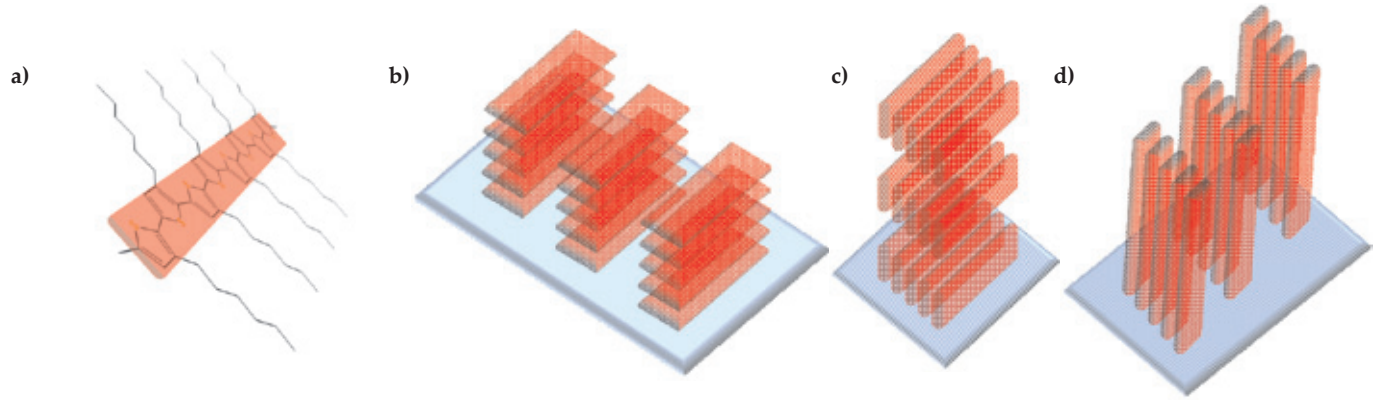

Fig. 3. Schematic representation: a) main chain of poly(3-hexylthiophene) (marked with a red ribbon), its possible orientation in crystalline structures on solid substrates (in blue) b) face-on, c) edge-on, d) perpendicular

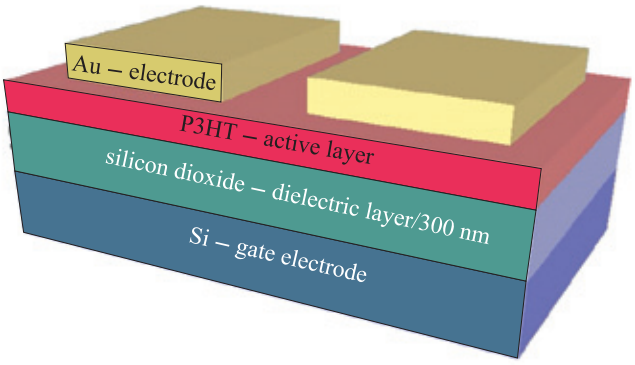

Fig. 4. Scheme of an ambipolar, organic field-effect transistor in bottom gate, top contacts configuration

is evident also for P3HT films with different orientational structures (Fig. 3). In the transistors, the holes are generally transported between source and drain (Fig. 4), *i.e.* the charge carrier transport is parallel to the film surface. Therefore, when P3HT chains are oriented *edge-on*, the direction of π-stacking (Fig. 3c) is in favor of the charge carrier transport [29]. In the case of a *face-on* oriented P3HT (Fig. 3b), the alkyl substituents form gaps between π-conjugated/π-stacked backbones and therefore hinder the charge transport in the direction parallel to the active layer [29].

The above simple relations between molar mass, crystalline structure and OFET performance, although generally true, are not as straightforward as they appear, because the polymers with different molar masses form crystals having distinctly different morphologies (Fig. 5). For example, films of P3HT with molar mass of 31.1 kg/mol exhibit a uniform, nodular morphology (Fig. 5b), but decreasing the molar mass of P3HT to 3.2 kg/mol leads to formation of a dense network of short rods (Fig. 5a). Although the layers obtained from P3HT with lower molar mass show higher crystallinity, the charge carrier mobility is lower. The mobility decreases since the crystalline rods are relatively short (~100 nm) and do not provide sufficient percolation paths for charge carriers due to high concentration of grain boundaries [29].

The morphology of P3HT films can be controlled not only by the molar mass of the polymer, but also by solvents used for deposition [30]. The variation in morphologies shown in Fig. 6 results mainly from the evaporation rates of the solvents. In the case of chloroform (boiling point ~61 °C) a typical nodular structure is obtained (Fig. 6a). When 1,2,4-trichlorobenzene (boiling point ~214 °C) is used, dense elongated aggregates are visible in the AFM image (Fig. 6b). This difference in morphologies has a direct consequence on the transistor performance: while the film spin-coated from chloroform reveals mobility of 0.012 $cm^2/V \cdot s$ the one obtained from 1,2,4-trichlorobenzene shows 0.12 $cm^2/V \cdot s$ [30]. It is therefore generally believed that fibrillar morphology provide more sufficient percolation paths for the charge carriers [30].

Current attention is drawn on physical methods to control the crystallinity and morphology of P3HT films in order to improve the charge transport. One promising and relatively simple technique is the controlled aggregation of P3HT in solution by ultrasonication [31] or UV irradiation [32].

POLY(3-HEXYLTHIOPHENE)/SMALL MOLECULE BLENDS

Formation of heterogeneous blends is a known strategy to modify properties of polymeric materials. In order to tailor electronic properties of P3HT-based devices, the polymer can be blended with small-molecular additives. The blending has been found either a way to enhance charge carrier mobility in the polymer [33] or a method to form transistors exhibiting both electron and hole type of charge transport in the active area by using a hetero-

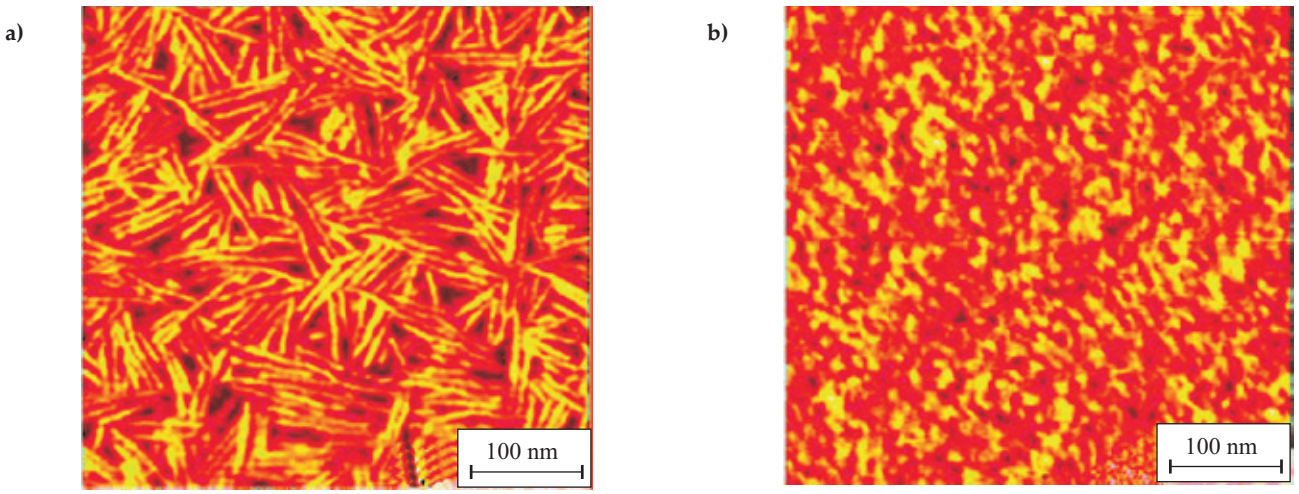

Fig. 5. Thin film morphologies of the spin-coated P3HT with: a) M_w = 3.2 kg/mol, b) M_w = 31 kg/mol; nanorods highlighted for better visualization (Figure adapted from [26])

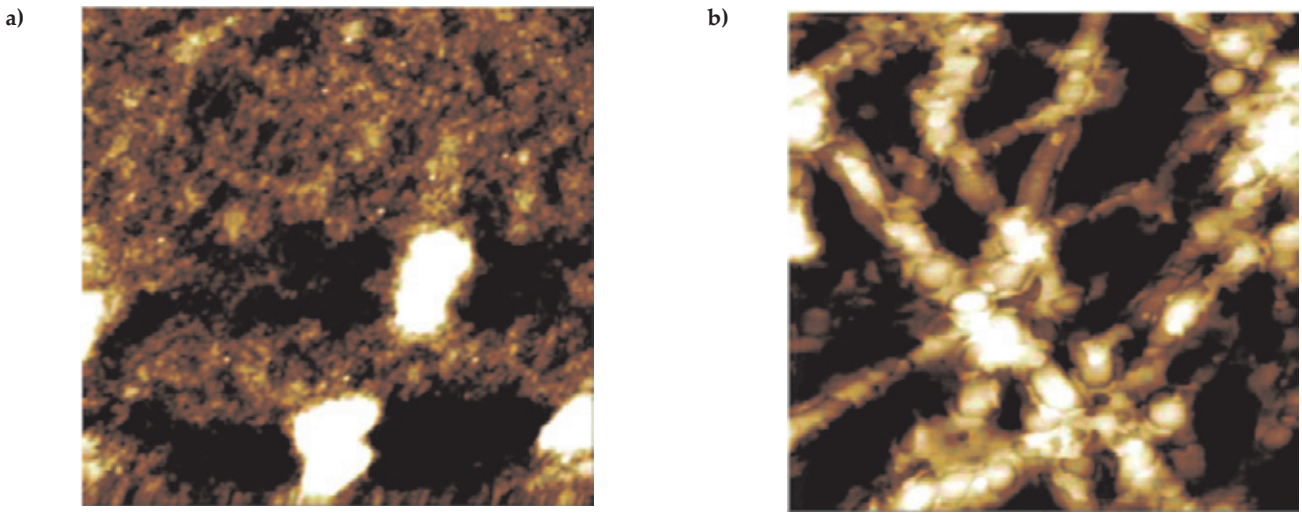

Fig. 6. Morphology of P3HT films obtained from: a) chloroform, b) 1,2,4-trichlorobenzene solutions (Adapted with permission from [28], Copyright 2004, American Chemical Society)

junction blend with an acceptor molecule [34]. The performance of devices based on P3HT blends depends on the crystallinity of the components and morphology of their organic active layers [35–37]. For the selection of the blend components, their interactions with P3HT has to be taken into account to control the phase separation in the film [38].

Alkylated derivatives of perylene diimides (PDI) are acceptor molecules which can be used for heterojunction blends with P3HT. PDI derivatives may affect formation of P3HT crystals. For instance (Fig. 7), in systems including dioctyl-perylenedicarboximide (PDI-3) and P3HT, (Fig. 7c) the polymer epitaxially crystallizes on PDI-3 fibrils and forms coaxial shish-kebab structures (Fig. 8) [39]. In such structures PDI-3 fibrils are the elongated cores of the disc-like P3HT crystals (Fig. 8). Crystal morphology in the P3HT:PDI-3 blends can be controlled by molar mass of the polymer, weight ratio of the components and type of solvent. Raising the P3HT ratio in the blend causes an increase in the number and length of P3HT fibrils in the blend, while the average diameter of PDI-3 fibrils drops. A decreased diameter of PDI-3 fibrils is also observed upon deposition from chloroform or chlorobenzene. An addition of a poor solvent to the P3HT:PDI-3 mixture in a good solvent (*e.g.* dichlorobenzene) causes a decrease in the average diameter of both PDI-3 fibrils and the disc-like, epitaxial P3HT crystals. Increasing the molar mass of P3HT decreases the diameter of PDI-3 fibrils and causes an increase in the diameter of epitaxial crystals of P3HT.

Morphology of P3HT blends with variable ratios of PDI derivatives shown in the Fig. 7a, 7b was reported by Puniredd *et al*. [34]. Both PDI-1 and PDI-2 derivatives ex-

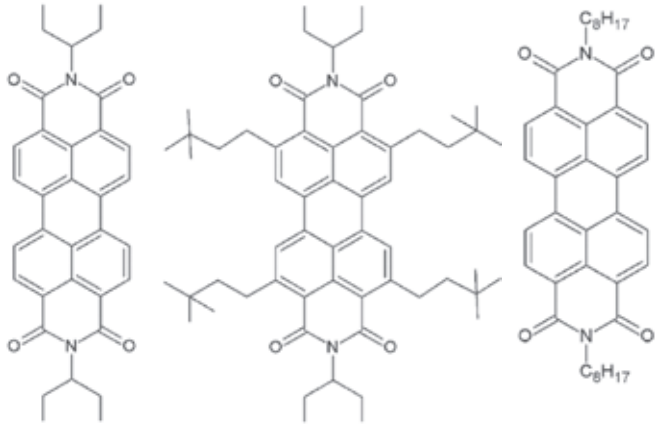

Fig. 7. Chemical structures of: a) PDI-1, b) PDI-2, c) PDI-3

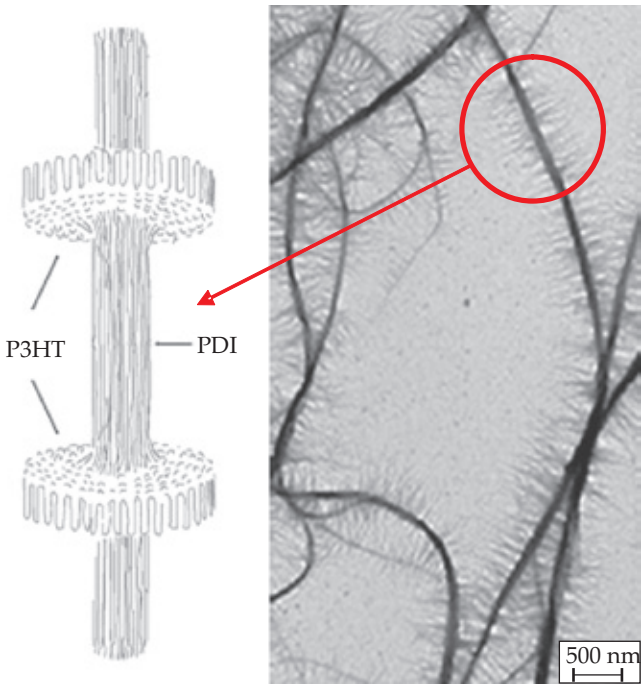

Fig. 8. Shish-kebab structures formed in the blends P3HT:PDI-3 (Adapted with permission from [37], Copyright 2012, American Chemical Society)

erted an influence on the surface arrangement of P3HT. In the film deposited under the same conditions as the blends, pure P3HT preferentially forms *face-on* oriented crystals. In blends with the PDI derivatives, however, an *edge-on* orientation is dominating. For the P3HT:PDI-1 weight ratios of 3:1 and 1:1 PDI-1 crystals in the blends are smaller than those of pure PDI-1. The morphology of PDI-1 crystals formed in the P3HT:PDI-1 1:3 blends was found nearly identical like in pure PDI-1. PDI-2 in the blends with P3HT always formed elongated, rod-like crystals irrespectively of the blend composition. Orientation of the crystals in the blends was, however, different for different compositions. When dominating in the blend, the PDI-2 crystals form vertical structures on top of the P3HT layer. In the case of P3HT:PDI-2 3:1 blends a diagonal penetration of the rod-like crystals through the entire film was observed. In the case of the PDI-1 small molecule crystals in these blends were formed on top of the P3HT layer irrespectively of the blend composition. Similar, vertical phase separation geometry was reported for blends of P3HT with hexylphenyl-bithiophene (dH-PTTP). In addition, moderate amounts of dH-PTTP have ability to nucleate crystallization of P3HT in the blends – increasing the content of dH-PTTP caused an increase in the crystallinity and a drop in the average crystal sizes of P3HT.

For the P3HT:PCBM (phenyl-C61-butyric acid methyl ester) blends it was reported that P3HT chains reorient at the interface when the blend is cooled from the melt [40]. Increasing the content of PCBM causes a decrease in the average size of P3HT crystals and at the 1:3 weight ratio no crystalline domains of P3HT were found in the blend. At the same time, a strong tendency for aggregation and ordering of PCBM is observed. In the blend P3HT:PCBM 1:3, PCBM forms distinctly aggregated and partly ordered domains. Blends of P3HT with synthetic graphene nanoribbons (GNR) have been also reported [41]. The addition of GNR strongly influences the crystallinity of P3HT. The amount of 2 wt % GNR dispersed in the P3HT matrix hinders the formation of coherent π-stacks. Increasing the GNR content above 2 wt % causes a notable decrease in lamellar order of P3HT, while the addition of above 5 wt % of GNR practically disables crystallization of P3HT. Above 5 wt % GNR in P3HT, the nanoribbons, similarly as PCBM, have a strong tendency to aggregate [41].

APPLICATION OF P3HT BLENDS IN ORGANIC FIELD-EFFECT TRANSISTORS

Application of P3HT blends has been considered a strategy to tune the OFET performance for more than a decade [42]. Addition of semiconducting small molecules to P3HT can lead to an increase in the hole mobility of P3HT in the active layer due to an improvement of the percolation path network between source and drain electrodes. Orgiu *et al*. [33] demonstrated that mixing P3HT with dH-PTTP improves the hole mobility of P3HT from 0.01 to 0.1 $cm^2/V \cdot s$. By addition of dH-PTTP to P3HT, crystalline assemblies of the small-molecule component bridged P3HT domains and therefore provided better percolation paths for the charge carriers. Similar improvements in the hole mobility were achieved by addition of graphene nanoribbons acting as additional percolation paths between crystalline domains of P3HT [41].

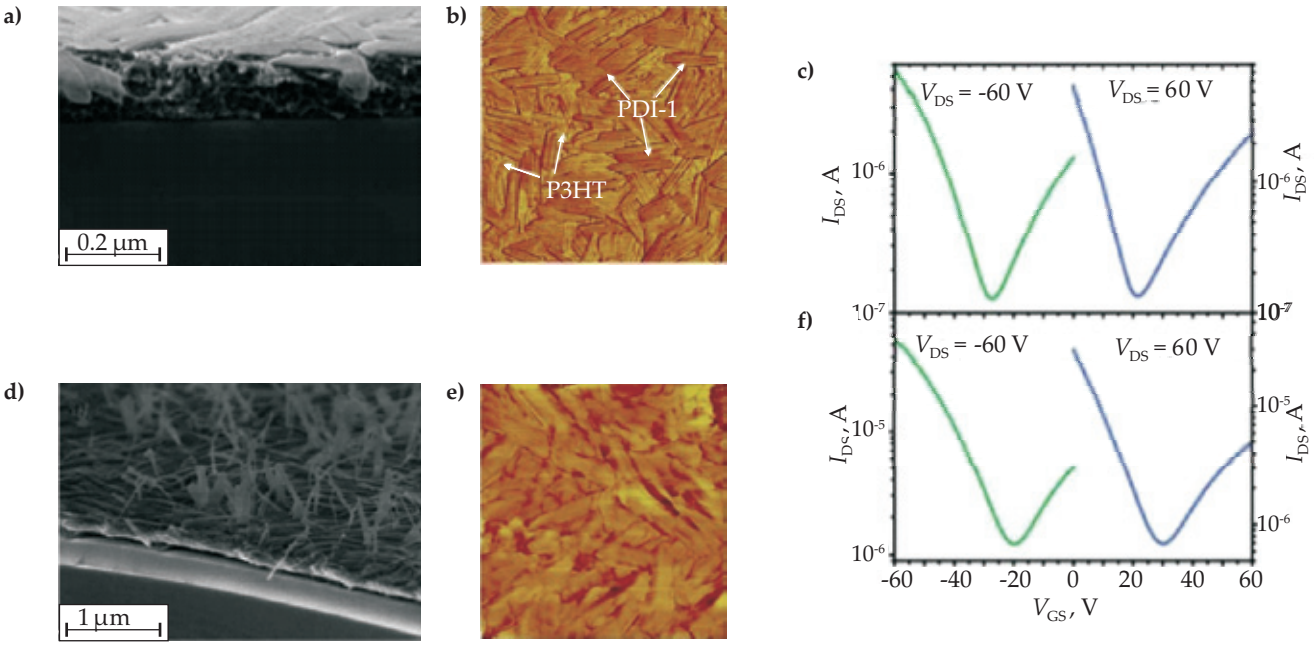

Fig. 9. AFM images (a, d), SEM cross-sectional images (b, e), OFETs transfer characteristics (c, f) of P3HT:PDI-1 active layers with weight ratios: a), b), c) 1:1, d), e), f) 3:1 ([32] Published by The Royal Society of Chemistry); G – gate, D – drain, S – source

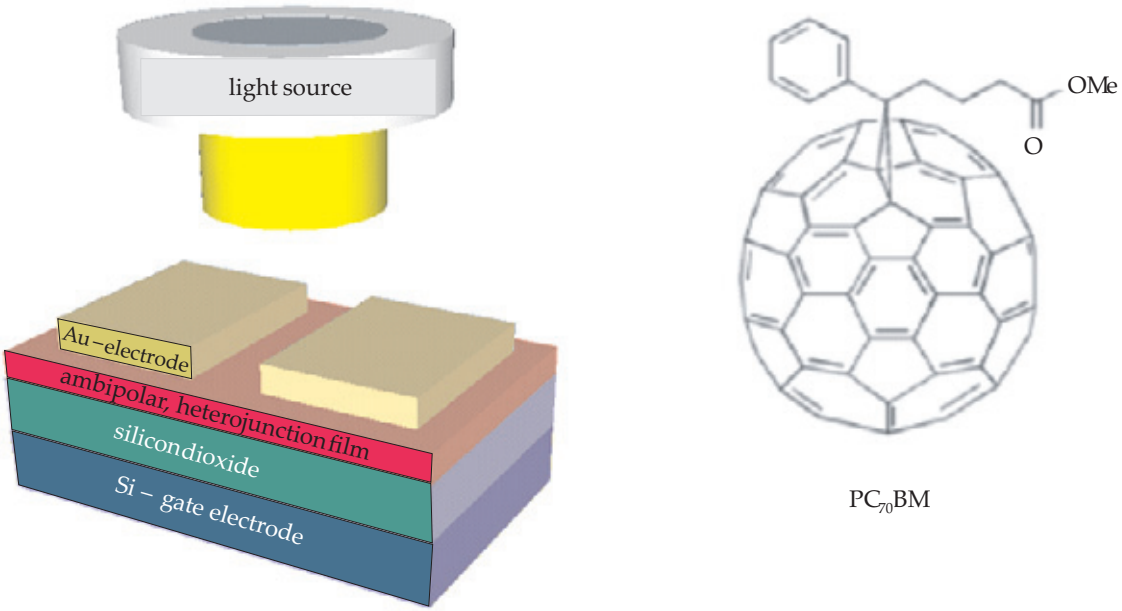

Fig. 10. Scheme of irradiated OFET device and chemical structure of $PC_{70}BM$

Blending P3HT (p-type semiconductor) with an additive revealing electron conductivity (n-type semiconductor) may lead to formation of layers having controllable transport of electrons and holes [34, 43, 44]. When the phase separation between the components results in formation of a heterojunction, the system can be considered a candidate for ambipolar OFETs [42, 45]. The ambipolar devices can be applied in complementary digital circuits where stable and comparable electron and hole transport in the active layer is necessary [44]. Furthermore, ambipolar transport can lead to light emitting organic transistors which opens the door towards large area flexible displays [46].

The ambipolar behavior of heterojunction OFETs can be tuned by varying the crystallinity and structure of the active layer [34]. As discussed previously, using different PDIs (PDI-1 and PDI-2) and varying the ratios of p-type to n-type components results in films with distinctly different morphologies as demonstrated in the exemplary AFM and SEM images (Fig. 9). As it can be concluded from the transfer curve profile (Fig. 9c), the films reveal an ambipolar behavior only when a horizontal phase separation between the polymer and PDI is observed. On the other hand, when PDI crystals were embedded in the polymer layer but not sufficiently interconnected, electron transport was severely hindered. In this case, however, the addition of PDI-2 caused an increase in the hole mobility of P3HT because of doping effects induced by the acceptor properties of small molecules.

Binary blends of P3HT and n-type small molecule in OFETs may also be used to investigate the photo-induced current and therefore provide valuable information for further development of organic photovoltaics [46]. Zheng *et al*. used ambipolar OFETs with active layers of P3HT and $PC_{70}BM$ fullerene to investigate the influence of light irradiation on electric current in the binary active layer (Fig. 10). The transistor operation significantly changes upon irradiation with an intensity of ~100 mW/cm^2. The photoresponse manifests as an increase in current between drain and source electrodes. Especially in the case of electron transport, the current increases almost one order of magnitude from 0.02 μA in dark to 0.14 μA upon irradiation. The authors explain these phenomena with photogeneration of electron-hole pairs in the heterojunction binary layer. Electrons or holes generated upon the light irradiation act as additional charge carriers in the conductive channel and therefore enhance the measured charge carrier mobilities.

Ambipolar OFETs consisting of binary blends of P3HT and small molecules still undergo an extensive research to understand the correlation between microstructure, phase separation, photosensitivity and ambipolar behavior [33, 41–48]. New compounds, methods of fabrication and applications of heterojunction binary blends of conjugated polymers and small molecules are in continuous development [33, 41–48].

ACKNOWLEDGMENT

This work was supported by National Science Centre, Poland through the grant 2013/08/M/ST5/00914. The authors would like to thank Prof. Jacek Ulański from Department of Molecular Physics, Lodz University of Technology for fruitful discussions.

REFERENCES

[1] Samitsu S., Shimomura T., Heike S. *et al*.: *Macromolecules* **2010**, *43*, 7891. http://dx.doi.org/10.1021/ma101655s
[2] Łużny W., Proń A.: *Synthetic Metals* **1997**, *84*, 573.
[3] Chen T.A., Rieke R.D.: *Journal of American Chemical*

Society **1992**, *114*, 10087.
http://dx.doi.org/10.1021/ja00051a066
[4] Trznadel M., Pron A., Zagorska M. *et al*.: *Macromolecules* **1998**, *31*, 5051.
http://dx.doi.org/10.1021/ma970627a
[5] Yokoyama A., Miyakoshi R., Yokozawa T.: *Macromolecules* **2004**, *37*, 1169.
http://dx.doi.org/10.1021/ma035396o
[6] Dudenko D., Kiersnowski A., Shu J. *et al*.: *Angewandte Chemie, International Edition* **2012**, *51*, 11068.
http://dx.doi.org/10.1002/anie.201205075
[7] Pascui O.F., Lohwasser R., Sommer M. *et al*.: *Macromolecules* **2010**, *43*, 9401.
http://dx.doi.org/10.1021/ma102205t
[8] Ludwigs S.: "P3HT Revisited – From Molecular Scale to Solar Cell Devices", Springer Berlin Heidelberg, Heidelberg 2014, pp. 39–82, 139–180.
[9] Prosa T.J., Winokur M.J., McCullough R.D.: *Macromolecules* **1996**, *29*, 3654.
http://dx.doi.org/10.1021/ma951510u
[10] Brinkmann M.: *Journal of Polymer Science, B Polymer Physics* **2011**, *49*, 1218.
http://dx.doi.org/10.1002/polb.22310
[11] Yuan Y., Shu J., Kolman K. *et al*.: manuscript in preparation
[12] Park Y.D.: *Bulletin of the Korean Chemical Society* **2014**, *35*, 2277.
http://dx.doi.org/10.5012/bkcs.2014.35.8.2277
[13] Wirix M.J.M., Bomans P.H.H., Friedrich H. *et al*.: *Nano Letters* **2014**, *14*, 2033.
http://dx.doi.org/10.1021/nl5001967
[14] Bielecka U., Lutsyk P., Janus K. *et al*.: *Organic Electronics* **2011**, *12*, 1768.
http://dx.doi.org/10.1016/j.orgel.2011.06.027
[15] Aryal M., Trivedi K., Hu W.: *ACS Nano* **2009**, *10*, 3085.
http://dx.doi.org/10.1021/nn900831m
[16] Liu J., Sun Y., Gao X. *et al*.: *Langmuir* **2011**, *7*, 4212.
http://dx.doi.org/10.1021/la105109t
[17] Sirringhaus H., Brown P.J., Friend R.H. *et al*.: *Nature* **1999**, *401*, 685.
http://dx.doi.org/10.1038/44359
[18] Bao Z., Dodabalapur A., Lovinger A.J.: *Applied Physics Letter* **1996**, *69*, 4108.
http://dx.doi.org/10.1063/1.117834
[19] DeLongchamp D.M., Vogel B.M., Jung Y. *et al*.: *Chemistry of Materials* **2005**, *17*, 5610.
http://dx.doi.org/10.1021/cm0513637
[20] Hintz H., Egelhaaf H.J., Lüer L. *et al*.: *Chemistry of Materials* **2011**, *23*, 145.
http://dx.doi.org/10.1021/cm102373k
[21] Jiang L., Zhang J., Wang W.: *Journal of Luminescence* **2015**, *159*, 88.
http://dx.doi.org/10.1016/j.jlumin.2014.11.002
[22] Sekine C., Tsubata Y., Yamada T. *et al*.: *Science and Technology of Advanced Materials* **2014**, *15*, 34203.
http://dx.doi.org/10.1088/1468-6996/15/3/034203
[23] Padinger F., Rittberger R.S., Sariciftci N.S.: *Advanced Functional Materials* **2003**, *13*, 85.
http://dx.doi.org/10.1002/adfm.200390011
[24] Jiang C., Cheng X., Wu X. *et al*.: *Optoelectronics Letters* **2011**, *7*, 30.
http://dx.doi.org/10.1007/s11801-011-0122-z
[25] Kuila B.K., Nandi A.K.: The *Journal of Physical Chemistry B* **2006**, *110*, 1621.
http://dx.doi.org/10.1021/jp055234p
[26] Chang H., Wang P., Li H., Zhang J., Yan D.: *Synthetic Metals* **2013**, *184*, 1.
http://dx.doi.org/10.1016/j.synthmet.2013.09.031
[27] Holliday S., Donaghey J.E., McCulloch I.: *Chemistry of Materials* **2014**, *26*, 647.
http://dx.doi.org/10.1021/cm402421p
[28] Tsao H., Müllen K.: *Chemical Society Reviews* **2010**, *39*, 2372. http://dx.doi.org/10.1039/b918151m
[29] Kline R.J., McGehee M.D.: *Journal of Macromolecular Science, Part C: Polymer Reviews* **2006**, *46*, 27.
http://dx.doi.org/10.1080/15321790500471194
[30] Chang J.-F., Sun B., Breiby D.W. *et al*.: *Chemistry of Materials* **2004**, *16*, 4772.
http://dx.doi.org/10.1021/cm049617w
[31] Hu H., Zhao K., Fernandes N. *et al*.: *Journal of Materials Chemistry C* **2015**, *3*, 7394.
http://dx.doi.org/10.1039/C5TC01425E
[32] Chang M., Lee J., Kleinhenz N. *et al*.: *Advanced Functional Materials* **2014**, *24*, 4457.
http://dx.doi.org/10.1002/adfm.201400523
[33] Orgiu E., Masillamani A.M., Vogel J.O. *et al*.: *Chemical Communications* **2012**, *48*, 1562.
http://dx.doi.org/10.1039/C1CC15477J
[34] Puniredd S.R., Kiersnowski A., Battagliarin G. *et al*.: *Journal of Materials Chemistry C* **2013**, *1*, 2433.
http://dx.doi.org/10.1039/C3TC00562C
[35] Günes S., Neugebauer H., Sariciftci N.S.: *Chemical Reviews* **2007**, *4*, 1324.
http://dx.doi.org/10.1021/cr050149z
[36] Peet J., Senatore M.L., Heeger A.J., Bazan G.C.: *Advanced Materials* **2009**, *21*, 1521.
http://dx.doi.org/10.1002/adma.200990046
[37] Brady M.A., Su G.M., Chabinyc M.L.: *Soft Matter* **2011**, *7*, 11065.
http://dx.doi.org/10.1039/C1SM06147J
[38] Buxton G.A., Clarke N.: *Physical Review B* **2006**, *74*, 85207. http://dx.doi.org/10.1103/PhysRevB.74.085207
[39] Bu L., Pentzer E., Bokel F.A. *et al*.: *ACS Nano* **2012**, *12*, 10924. http://dx.doi.org/10.1021/nn3043836
[40] Verploegen E., Mondal R., Bettinger C. J. *et al*.: *Advanced Functional Materials* **2010**, *20*, 3519.
http://dx.doi.org/10.1002/adfm.201000975
[41] El Gemayel M., Narita A., Dössel L.F. *et al*.: *Nanoscale* **2014**, *12*, 6301.
http://dx.doi.org/10.1039/c4nr00256c
[42] Babel A., Jenekhe S.A.: *Macromolecules* **2004**, *37*, 9835.
http://dx.doi.org/10.1021/ma0482314
[43] Kim F.S., Ahmed E., Subramaniyan S., Jenekhe S.A.: *ACS Applied Materials and Interfaces* **2010**, *11*, 2974.

http://dx.doi.org/10.1021/am1006996
[44] Szendrei K., Jarzab D., Chen Z. *et al*.: *Journal of Materials Chemistry* **2010**, *20*, 1317. http://dx.doi.org/10.1039/B919596C
[45] *Pat. US* 6 815 711 B2 (2014).
[46] Zhang Y., Liu J., Nguyen T.-Q.: *ACS Applied Materials and Interfaces* **2013**, *5*, 2347. http://dx.doi.org/10.1021/am302833j
[47] Zhou X., Ai N., Guo Z.-H. *et al*.: *Chemistry of Materials* **2015**, *27*, 1815. http://dx.doi.org/10.1021/acs.chemmater.5b00018
[48] Lu C., Wang J., Chang H.-C. *et al*.: *Journal of Materials Chemistry C* **2014**, *2*, 7489. http://dx.doi.org/10.1039/C4TC01267D